

Indirect selective laser sintering of gas and water atomized Stainless Steel (SS) powders

José Maria Mascheroni, jose@alkimat.com.br¹

Cristiano Binder, cristiano.binder@ufsc.br²

Matheus Grande de Aguiar, matheus.graguiar@gmail.com^{1,2}

¹ Alkimat Tecnologia Ltda. – Rua Abelardo Manoel Peixer, 142. 81110 – 055.São José, SC – Brasil

² Laboratório de Materiais – Universidade Federal de Santa Catarina. Rua Delfino Conti. 88040-370 - Bloco B, Engenharia Mecânica UFSC - Trindade, Florianópolis – SC.

Abstract. *Indirect Selective laser sintering (SLS) of metals is an alternative process to produce free form parts against direct Selective laser melting (SLM) process. In an indirect method of SLS process, “green parts” can be formed through selectively fusing a polymer binder to bond metal particles with a low power CO₂ laser. The polymer binder is subsequently removed and the polymer-free part (“brown part”) is then sintered or further processed to form a finished part. Stainless steel (SS) powders are widely used in powder metallurgy industry and are produced by two common techniques: gas atomization and water atomization. Gas atomization yields spherical particles and water atomization gives irregular particles. The density of the powder bed depends on particle packing density which is influenced by particle characteristics, such as size and shape. Selection of suitable power is a promising strategy to increase the sintered density without sacrificing any benefits of free form fabrication. In the present work, a Brazilian designed and manufactured SLS equipment, with a CO₂ laser, were employed for study the densification of indirect selective laser sintered metal parts, fabricated by a mixture of Nylon-12 matrix and SS gas and water atomized powder, mechanically mixed. The aim is to understand the effects of the particle size and morphology on part densification and mechanical properties. The powder characteristics are examined by scanning electron microscope (SEM) and laser diffraction particle size analysis. After sintering in a plasma reactor, the pores sizes and porosity percent of both mixtures were evaluated. Further investigations are planned into post-processing, such as binder decomposition and high-temperature sintering, of the green parts made from the powders mixture.*

Keywords: *Selective Laser Sintering, Indirect, Stainless steel*

1. INTRODUCTION

Selective laser sintering (SLS) is an advanced additive manufacturing technology, which can shorten the manufacturing time cycle, hence reducing the production cost and increasing competitiveness, and directly forms solid components according to a three-dimensional Computer-aided design (CAD) model by selective sintering of successive layers of powdered raw materials (Kumar, 2003; Kruth et al., 2003). SLS of metals is divided into indirect and direct methods. The direct SLS process melts the metal powders directly without any binder and eliminates the need for post-processing. While the capability of SLS to produce functional objects directly from metals is still under development, indirect methods of producing functional objects from metals have also been widely used (YAN, C. Z. et al, 2009a).

In an indirect method of SLS process, green parts can be formed through selectively fusing a polymer binder to bond metal particles with a smaller power laser. The polymer binder is subsequently removed, usually by thermal processes, and the polymer-free part is then sintered or further processed to form a finished part with geometric precision that is comparable to that of the green part. It is important that the green parts show sufficient mechanical properties to retain the desired shape and dimensions during handling and post-processing.

Stainless steel (SS) powders are widely used in powder metallurgy industry and are produced by two common techniques: gas atomization and water atomization. Gas atomizations yields spherical particles, or close to spherical, and provide good flowability and tap density in SLS processing. Water atomization gives irregular particles that provide a good green strength of the cold compacted powders (Thummler, F. et al., 1993).

At present, two methods have been used to produce polymer binder/metal composite powders for the indirect SLS process. The first method is that the polymer binders uniformly coat metal powders. The coated composite powders are widely used for the relatively lower binder content and higher binder efficiency. The other method to produce polymer binder/metal composite powders for the indirect SLS process is to mechanically mix metal powders with polymer binder powders. In general, the mixed composite powders are not commercially viable due to problems associated with powder segregation during shipping and with poor binder efficiency (Beaman et al., 1997).

One way to increase green part strength would be simply to increase the amounts of polymer binders. However, as the binders are removed by thermal processes, void spaces are left behind. High contents of polymer binders result in relatively larger amounts of void spaces upon high-temperature sintering, which can lead to unacceptable amounts of shrinkage in the finished part (Yan, C.Z. et al, 2009a). Another problem with incorporating high content of polymer binders requires longer annealing times to remove the binder, which obviously reduces efficiency and add costs.

Ruidi Li (2010), conducted a detailed study to investigate the densification behavior of gas and water atomized 316L stainless steel powder via direct selective laser sintering process, or Selective laser melting, and found that samples fabricated from gas atomized powder possesses a denser, because of the lower oxygen content in gas atomized powder and attendant better wetting ability for SLS process. Also, the higher packing density of gas atomized powder is another reason for the higher densification behavior of gas atomized powder.

The purpose of the present study is to prepare gas and water atomized 316L stainless steel (316L SS) parts by indirect SLS process. The aim is to understand the effects of both different powders on part densification, surface morphology and shrinkage rate, using the same mixture and processing SLS parameters.

2. EXPERIMENTAL PROCEDURES

2.1. Materials

In this work, two kinds of powders of gas atomized and water atomized 316L stainless steel were used. The gas atomized powder, purchased by Höganäs, has a spherical shape, with the particle size distribution of 3–40 μm and the mean particle size of 20 μm . The water atomized powder, provided by BRATS, has an irregular shape, with the particle size distribution of 20–53 μm and the average particle size of 29 μm .

The polymer binder used was the Polyamide 12 (nylon-12) powder, obtained from BRASKEM in Brazil. The properties of the nylon-12 according to its specification are listed in Table 1. Selecting nylon-12 as the polymer binder for the indirect SLS process was largely governed by the previous works, which suggested that nylon-12 SLS parts have relatively high densities and strengths, and nylon-12 has good interfacial adhesion with metals.

Table 1 - Properties of the nylon-12 according to its specification (Data-sheet Braskem)

Property	Test Method	Nylon-12
Melting temperature ($^{\circ}\text{C}$)	DSC	181 < $_$ < 185
Average Particle Size (μm)	Laser Diffraction	38 < $_$ < 48
Part Density – 23 $^{\circ}\text{C}$ (g/cm^3)	ExcelTec Method	0.98 \pm 0.05
Tensile strength (MPa)	ISO 527	44 \pm 1
Charpy notched impact strength (KJ/m^2)	ISO 179	6 \pm 0.5

Particle size of the water and gas atomized stainless steel powder was determined using a Cilas 1190 laser particle size analyzer, with liquid dispersion, which uses a laser diffraction to measure the size of particles. In this method the intensity of light scattered is measured by a laser beam passes through a dispersed particulate sample. The size distributions were reported by the cumulative volume diameter at 10%, 50% and 90% and demonstrated in the table 2 below:

Table 2 – Both stainless steel powders size distribution.

Stainless steel powder	Supplier	D ₁₀ (μm)	D ₅₀ (μm)	D ₉₀ (μm)	D _{av.} * (μm)
Water atomized	Brats	14.78	27.63	48.34	29.9
Gas atomized	Höganäs	28.35	41.51	60.46	43.16

*d_{av.}: Average diameter

2.2. Powder preparation

The mixture of the polyamide 12 with gas atomized and water atomized stainless steel powders were performed by a Y-mixer provided by Laboratório de Materiais from Federal University of Santa Catarina. In the Y-mixer, during the first rotation the powder falls down into the two arms of the mixer. Part of the mixing action arises from the diversion of the original amount of powder into the two arms which then converge turbulently on the second inversion of the mixer as the powder pours back into the bottom of the system (Kaye, B.H., 1997). The content of nylon-12 in both mechanically mixed mixtures of stainless steel and nylon powder were 8%, in weight. Each SS powder was mixed with PA12 for an hour with a 30 rpm of rotation speed.

2.3. Processing

The SLS process was performed by LASERFUNDE (Fig. 1), a home designed and developed SLS equipment, developed by Alkimat Tecnologia Ltda.. The SLS machine is equipped with a CO₂ laser (wavelength of 10.6 μm) and F-theta lens systems. The fabricating space of the machine was 120mm (L)×120mm (W)×100 mm (H). Moreover, the processing chamber of this equipment can be vacuumed and then protected from oxidation by controlling the atmosphere.

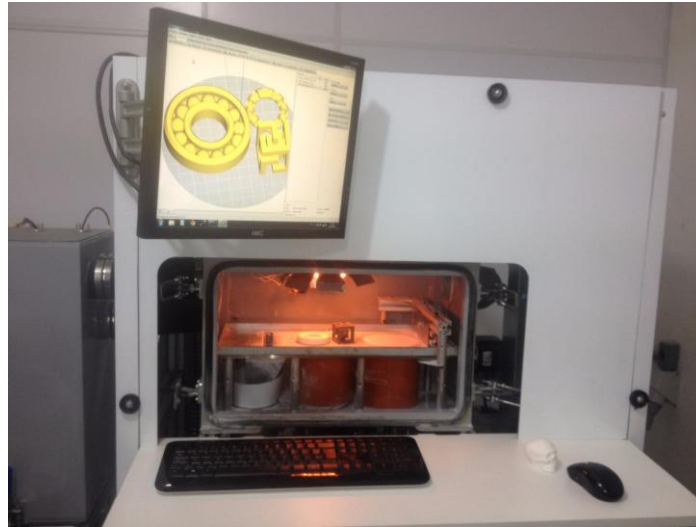


Figure 1 - SLS 3D Printer LASERFUNDE, developed by Alkimat Tecnologia Ltda.

The figure below shows the LASERFUNDE SLS equipment fabricating a SS/PA12 cube. The fresh powders were delivered through a powder feeding apparatus; a warm-up time of 30 minutes was given before the processing.

Energy density (ω), defined as the relative applied laser energy per unit area, can be calculated by equation (1) (Ho et al., 1999):

$$\omega = \frac{P}{H \times v} \quad (1)$$

Where P is the fill laser power, H is the scan spacing, and v is the laser beam traversing speed. In this work, v was 1000 mm/s; H was 0.25 mm; P was 60W. Therefore, the energy density was 0.24 J/mm². The part bed temperature was 90°C in the center of the platform and the powder layer thickness was 0.25 mm. All test specimens were fabricated using the scanning method that scans each successive layer in alternate, perpendicular directions.



Figure 2 – LASERFUNDE SLS equipment fabricating the SS/PA12 cubes.

In each polyamide 12 powder mixture using metallic powders fabricated using different atomization processes (gas and water atomization), three cubes with 15x15x15 mm size were manufactured. One cube of each was selected to morphology analysis in scanning electron microscope (SEM) and in all parts dimensional measurement and relative post-sintering density were executed.

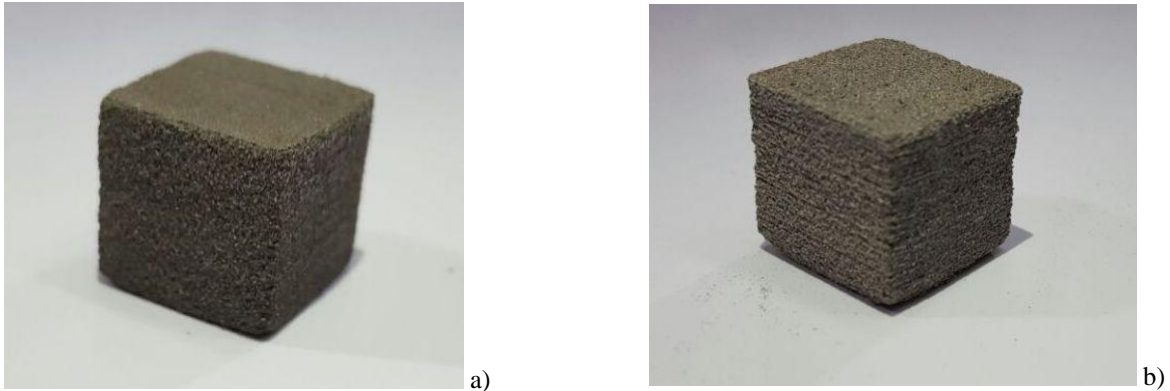


Figure 3 – Stainless steel/polyamide-12 cubes fabricated with: a) water atomized SS; b) gas atomized SS.

2.4. Post-processing

After the process of building a fragile green part from mixed 316 stainless steel powders held in a polyamide 12 matrix, the post-processing of SLS process comprised thermal debinding and subsequent sintering, which were continuously conducted in an Plasma assisted debinding and sintering (PADS) reactor (Binder, C., 2009). In this step the green parts were placed into the PADS with 400V of voltage and 1 Torr pressure. During the heating phase the polymer was burned away leaving the steel skeleton, which was then sintered traditionally to a porous steel structure. According to the plasma assisted debinding and sintering, the heating rate was 5 °C/min from room temperature to 300°C and 0.7°C/min for 300°C to 500°C, with a hydrogen flow of 1000 cm³/min until 500°C. After that, the binder-free parts were sintered at a heating rate of 5°C/min from 500°C to 1200°C and maintained for 1 h at 1200°C. After 500°C the reactor flow were kept in 500 cm³/min of a mixture containing 95% of argon (99,999% purity) and 5% hydrogen (99,995% purity). The sintered parts were kept inside the reactor for 3 hours for cooling and then the reactor was open and the parts cooled in air.

2.5. Characterization

Microstructure and surface morphology of the stainless steel mixed with Nylon-12 cubes was examined using a JEOL JSM-6390LV scanning electron microscope at an accelerating voltage of 15 kV, provided by Laboratório de Materiais from Federal University of Santa Catarina. In order to prepare a sample for examination, a sample holder with an adhesive tape mounted on, was glued to a piece of the SS part. The piece was bent until fracture, at room temperature. Sample was gold sputtered before the examination.

The relative sintered densities were measured in a METTLER TOLEDO XS205 Dual Range Analytical Balance. For this characterization, the 15x15x15 mm cubes were soaked in a paraffin wax to cover and isolate the open porosity, and weighed before and after the soaking.

3. RESULTS AND DISCUSSION

3.1 Dimensional Accuracy

As the “Laserfunde” SLS equipment is home developed, the accuracy in fabrication of parts is a point that must be considered and measured. During the printing of the composite cubes, two main dimensional problems can occur. The first issue is the building accuracy of the equipment and the second one is the formation of part growth (in this work, named “part cake”). The building accuracy is an issue that occurs due to the equipment precision on laser sintering and on height of each deposited layer. As the equipment is set to come down a layer height value, which in the case of this work is 0.2 mm, whether the building platform slow down a value close to this height in each layer, in the end of building the Z-axis dimensional could be different of that settled.

This may be due to a phenomenon referred to as part growth in the SLS process, which is schematically shown in Figure 4. In the SLS process, the sintered part has a higher temperature relative with the surrounding loose powder. Therefore, thermal energy stored in the sintered part propagates outward into the surrounding loose powder and raise local temperatures, as shown in Figure 4(a). When the temperature of surrounding powder is elevated beyond the caking temperature, which is T_m for semi-crystalline polymers, an uncontrolled or secondary sintering layer that resides adjacent to the surface of the desired part geometry is generated (as shown in Figure 4(b)), and thus part cake happens. Part cake causes the increase in the dimensions of SLS parts. The larger energy density, the more serious part growth happens, because increasing energy density can enlarge the temperature gradient between the sintered part and the

surrounding powder. Therefore, the dimensional errors increase with the increase in energy density. (Yan, C. et al., 2009b).

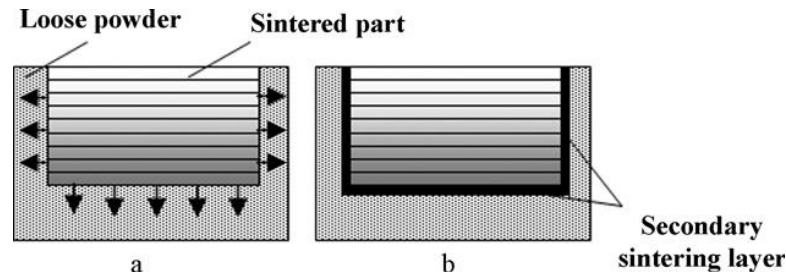


Figure 4 - Schematic illustration of part growth (part cake) in the SLS process. (YAN, C. Z., 2009b).

It is known that in the thermal cycle of sintering, the metal parts shrink significantly, due to the fact that the part is during heating degrading the binder element that is boiling and converting in to gas. This gas is being expelled of the structure by the same time the metal particles are forming necks to each other and starting to sinter. Subsequently the total removal of the part binder, the metal particles starts to sintering exponentially according to the increase in temperature and the binder-free metal part begins to densify, which causes a shrinkage in the part dimensions.

The dimensional variations in the X, Y and Z axes and the volumetric variations of the green and sintered parts are shown in table 3 below. The dimensional variations of the green part are in relation to the dimensional set for the cubes, which is 15x15x15 mm, and the variation of the sintered parts is compared to the dimensional found in the green parts. Thereby, we can obtain the accuracy of the equipment and the percentage of shrinkage of the material according to the amount of binder and the sintering temperature employed.

Table 3 – Dimensional deviation of green and sintered cubes.

	Average dimensional deviation (%) in axis:						Volumetric deviation (%):	
	X		Y		Z		green part	sintered part
	green part	sintered part	green part	sintered part	green part	sintered part		
SS - Gas atomized	1,83%	-6,19%	0,50%	-9,55%	-0,83%	-3,53%	1,49%	-18,14%
SS - Water atomized	1,33%	-9,08%	3,11%	-7,15%	-2,44%	-7,94%	1,95%	-22,26%

It can be seen that the dimensional errors change from the positive errors of the green parts to negative errors of the binder-free parts, indicating that shrinkage of the cubes occur throughout the manufacturing process. As said before, the shrinkage can be attributed to the complete loss of the binder, sintering of the metal particles and densification of metal parts.

The results in the table above, exhibits that there has been a positive variation in X and Y axes in both powders due to the formation of little “part cake”, and a negative variation in Z due to imprecision of the equipment. The higher negative variation in Z axis occurred in the atomized water cubes, which is believed to have been influenced by the poor quality of powder flow that formed lacks of powder filling in the layers, generating a lower part. Nevertheless the volume of the green parts had an increase in value when compared to the cubes with 15mm edge.

In the sintered parts, occurred an evident shrinkage in the three axes, which consequently generated a negative volumetric deviation of 18.14% for the gas atomized stainless steel and 22.26% for the water atomized SS, when compared to the green parts. It is believed that the greater shrinkage of the water powder part is due to its higher densification rate during sintering. In both cases the pieces shrank more significantly in the X and Y axes, which are parallel to the manufacturing layers indicating a greater sintering between the particles of each layer than a bonding between consecutive layers.

3.2 Relative Density

The temperature on the selective sintering process has been kept in 90°C in center of the building platform, which is a relatively low process temperature when compared with the nylon-12 selective sintering that is above 140°C. This value of temperature was fixed due to the non-homogeneous poor powder flowability to the building platform in higher temperatures specially observed in the water atomized stainless steel.

Fangxia Xie et al. (2013) have shown the effect of sintering temperature on the porosity of as-sintered 316L SS (Fig. 4.) It is distinct that the porosity of the sintered samples is affected by sintering temperature to a great extent. With a rise in sintering temperature, the total porosity drops steadily, while the open porosity falls drastically. The variation of the closed porosity with sintering temperature can be judged by the distance between the total and open porosity. It is

found that the distance increases with sintering temperature, namely the closed porosity goes up remarkably. According to this figure, after sintering at 1200 °C, the specimens possess a total porosity of 41% and the open porosity, a measure of pore interconnectivity, of 30%, indicating that there is a closed porosity of 11%, by calculation.

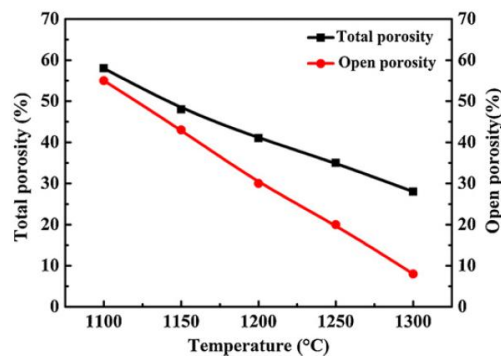


Figure 5 - Effect of sintering temperature on porosity of 316L SS parts. (Fangxia Xie et al., 2013)

In principle, the post-heating process of SLS green parts follows the traditional isothermal sintering of powders. At the early stage of heating, the binder decomposes slowly up to thorough burnout, and meanwhile the metallic particles contact together and connect gradually to form sintering necks. As the sintering temperature elevates, the massive atoms migrate towards the connective surfaces, which makes the sintering necks grown and the interparticle spacing shorten, so that both the pore size and the porosity reduce. A further increase in sintering temperature causes the closure of open-cellular pores and a small amount of shrinkage occurs (Fangxia Xie et al., 2013).

The main difference in both water and gas atomized SS powders is that the stainless steel cooled with water during the atomization process result in quite different particle shapes, sizes and surface morphology. Irregular particle shapes provide a normal green strength but as a result of the shear stresses between the particles each other, with the spreader and the platform the flowability is not homogeneous, so the powder deposition is not a homogeneous sheet, or layer. In consequence, the particle density in the deposition is not good. In the gas atomization process, the particles shape is spherical, or close to spherical, which gives an advantage in a higher green density as a result of homogeneous and easier powder flowability to the platform of fabrication, yielding a better arrangement of the particles.

However in the thermal sintering and debinding process, the processing difficulties related to the particle shape are the opposite. Irregular shapes are better in the process of debinding/sintering because their irregularities that anchor to each other and the contact area between the particles is large enough to keep the particles together allowing an easier and more numerous formation of necks. The spherical particles usually have smaller contact area due to its circular shape, which restricts the anchoring between the particles.

Posterior the thermal cycle is complete, the steel sintered cubes densities were measured in an Archimedes balance. For this characterization, the cubes were soaked in a paraffin wax to cover and isolate the open porosity, and weighed before and after the socking. The relative density average measured in the three different cubes of each material is related in the Table 4 below.

Table 4 – Relative density of the sintered cubes

SS Cubes:	Relative density (g/cm ³)
Gas atomized	3.95
Water atomized	2.84

As can be seen, the gas atomized cubes have higher values of relative density when fabricated by the same conditions and processes. Although, the spherical shape restricts the contact area and reduce the neck formation of particles, the cubes relative densities, when fabricated by the same conditions and processes, have higher values in the gas atomized. This is correlated due to the better deposition of gas powder in the SLS process, which gives a better particles packing in the green part that probably also have higher densities than the water powder.

Compared to the real density of these materials that is close to 8g/cm³, the values obtained are low. However, the explanations for these low densities are associated to the high volumetric percentage of binder (nylon-12) and the relatively low sintering temperature. Usually, stainless steel is sintered in 1350 Celsius degrees, so 1200° C is a low condition, that, as the figure 5 showed, really interferes in the part porosity and in consequence in the relative density.

3.3 Surface Morphology

The scanning electronic microscope (SEM) micrographs of the water and gas atomized stainless steel cubes are shown in figure 7. The surfaces parallel and perpendicular to the direction of powder deposition in building layers were analyzed. These surfaces are indicated in the figure below.

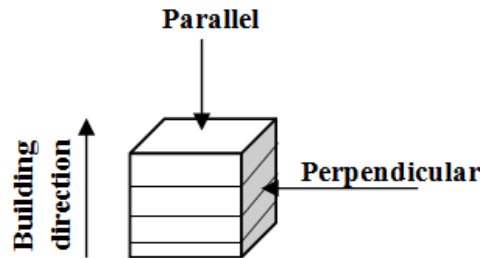


Figure 6 – Illustration of the surfaces parallel and perpendicular to the construction direction of the cubes.

The porosity size and distribution in both water and gas atomized sintered cubes are not homogeneous. That is justified by the non-homogeneous deposition of powder when building the parts and, since there is a big difference in density between the neat nylon-12 and stainless steel powders, it is very difficult to uniformly disperse the binder particles in the metal matrix by the mechanically mixing method. (Yan, C. Z. et al., 2009a).

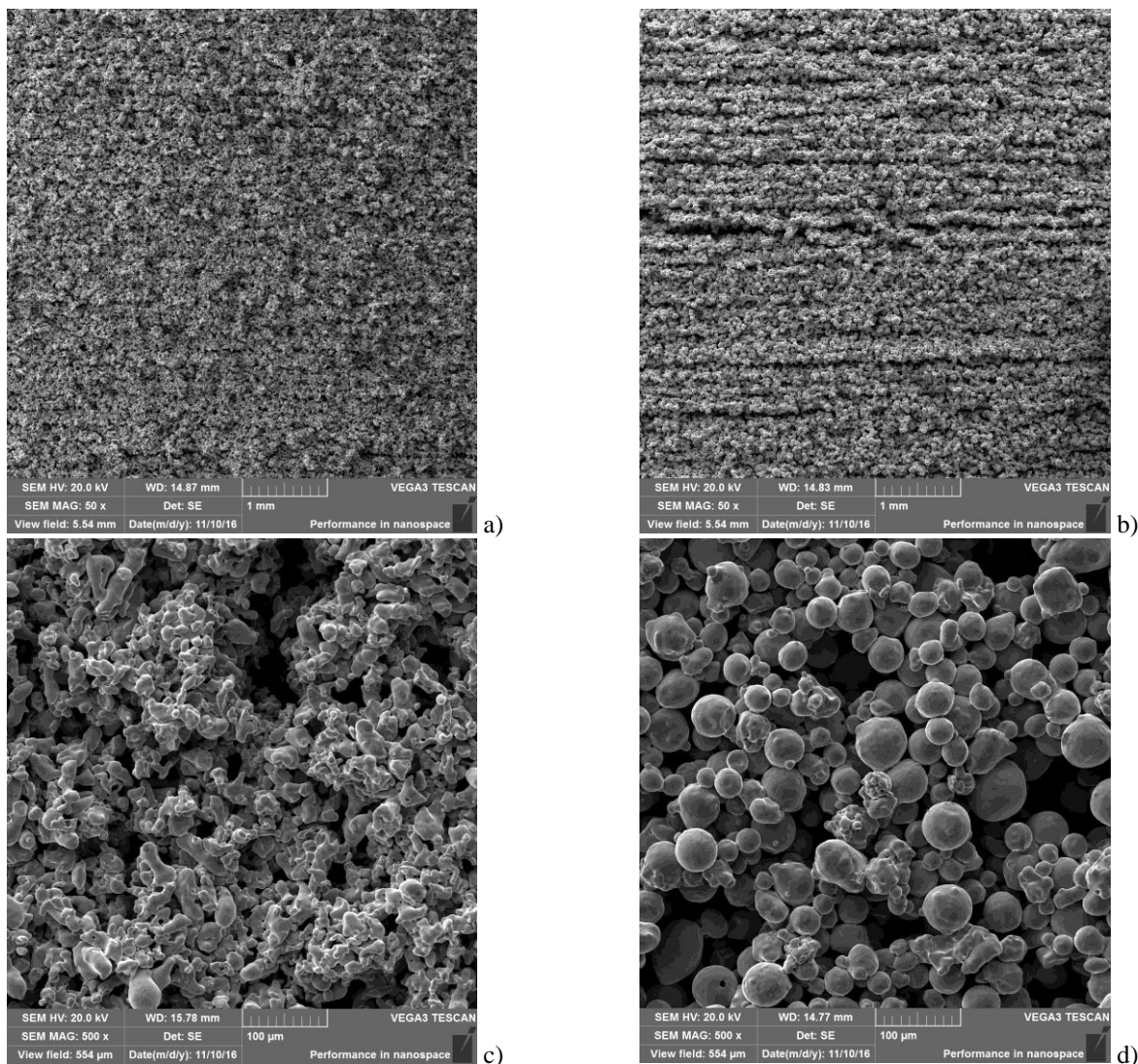


Figure 7 – SEM micrographs of the stainless steel cubes using: a) and c) water atomized powder; b) and d) gas atomized powder. Magnification - a) and b): 50x (perpendicular surface); c) and d): 500x (parallel surface).

Solid metal particles bond to each other forming a network of columnar agglomerates that represent the laser scan line and are separated by longitudinal gaps that represent the building layers. However, the sintered surfaces consisted of a network of equiaxed agglomerates and inter-agglomerate pores (Niu, H.J. et al., 1999). That same description of structure is found in those figures above, which in between the agglomerates the pores appeared open and deep.

The water atomized SS powder particles have slightly finer particles, as showed the table 3, with higher surface area per unit volume and therefore they can absorb more thermal energy, leading to an enhanced sintering kinetics. However, nonspherical particles give a lower random packing density and coordination number than spherical particles (German, R. M., 1989).

On parallel surface to the manufacturing direction, the gas atomized steel cubes were better sintered, with lower porosity and smaller and more distributed pores, as well as the water atomized steel cubes had a slightly higher amount of porosity. Fig. 6 c) and d) exhibits a discontinuous surface with many visible pores. Due to the high amount of binder volume and the low sintering temperature, as previously mentioned, the part structure remained intact, although with a large volume of porosity. It is believed that values close to those indicated in figure 5 on the article have been reached. In more detail, a high-magnification SEM image shows that a large amount of small metallic balls were present on the sample surface (figure 7(d)).

Analyzing the perpendicular surfaces, shown in figure 7 a) and b), the atomized water cube sintered better, when compared to the gas atomized cubes, due to a better anchoring of the particles and having slightly smaller particles. In the gas atomized was possible to clearly see the layers of fabrication that did not get so tight to each other during sintering. Despite this, the gas SS cube has remained denser as shown earlier and we believe this is due to the better packaging and distribution of the gas atomized SS powder in the manufacturing bed.

4. CONCLUSIONS

This work is a detailed study conducted to investigate the difference on dimensional accuracy, part densification and surface morphology of indirect selective laser sintering of stainless steel atomized using water and gas as the vehicle for the dispersion of particles. The conclusions take from this work are:

- The dimensional measurement indicates that shrinkage of the cubes occur throughout the manufacturing process, due to the complete loss of the binder, sintering of the metal particles and densification of metal parts. The green parts had an increase in volume when compared to the cubes with 15mm edge. The sintered parts, generated a negative volumetric deviation of 18.14% for the gas atomized and 22.26% for the water atomized SS, when compared to the green parts.
- The sintered stainless steel cubes reached relative density of 3.95 g/cm³ for gas atomized steel and 2.84 g/cm³ for water atomized. Although, the spherical shape restricts the contact area and reduce the neck formation of particles, the gas atomized cubes have higher values of relative density when fabricated by the same conditions and processes, when compared to the gas atomized.
- All sintered cubes presented porosity size and distribution non-homogeneous. Due to the high amount of binder volume and the low sintering temperature, all cubes remained intact, but with a large volume of porosity. On parallel surface to the manufacturing direction, the gas atomized steel cubes were better sintered, with lower porosity and smaller and more distributed pores. Analyzing the perpendicular surfaces, the atomized water cube sintered better, when compared to the gas atomized cubes, due to a better anchoring of the particles and having slightly smaller particles.

It is suggested that in future works the manufacturing through indirect sintering of metals with less use of polyamide-12 as the binder, and higher sintering temperatures, aiming for parts with less porosity and greater mechanical resistance, that can be used in mechanical applications. Cubes like those obtained in this work can be used in applications where high porosity and low mechanical strength is required, such as metal filters.

5. REFERENCES

- Beaman, J.J., Barlow, J.W., Bourell, D.L., Crawford, R.H., Marcus, H.L., McAlea, K.P., 1997. Solid Freeform Fabrication: A New Direction in Manufacturing. **Kluwer Academic Publishers**, Boston.

- BINDER, Cristiano. **Desenvolvimento de novos tipos de aços sinterizados autolubrificantes a seco com elevada resistência mecânica aliada a baixo coeficiente de atrito via moldagem de pós por injeção**. 2009. Tese de Doutorado. Universidade Federal de Santa Catarina, Centro Tecnológico, Programa de Pós-Graduação em Ciência e Engenharia de Materiais, Florianópolis.
- Ho, H.C.H., Gibson, I., Cheung, W.L., 1999. Effects of energy density on morphology and properties of selective laser sintered polycarbonate. **J. Mater. Process. Technol.** 89-90, 204–210.
- KAYE, Brian H. **Powder mixing**. Springer Science & Business Media, 1997.
- LI, Ruidi et al. Densification behavior of gas and water atomized 316L stainless steel powder during selective laser melting. **Applied Surface Science**, v. 256, n. 13, p. 4350-4356, 2010.
- NIU, H. J.; CHANG, I. T. H. Selective laser sintering of gas and water atomized high speed steel powders. **Scripta Materialia**, v. 41, n. 1, p. 25-30, 1999.
- GERMAN, R.M. **Particle Packing Characteristics**, p. 122, Metal Powder Industries Federation, Princeton, NJ (1989).
- THUMMLER, Fritz; OBERACKER, Rainer. Introduction to powder metallurgy. **Oxford Science Publications**, 1993. **346**, 1993.
- XIE, Fangxia et al. Structural and mechanical characteristics of porous 316L stainless steel fabricated by indirect selective laser sintering. **Journal of Materials Processing Technology**, v. 213, n. 6, p. 838-843, 2013.
- YAN, C. Z. et al. Preparation and selective laser sintering of nylon-coated metal powders for the indirect SLS process. **Rapid Prototyping Journal**, v. 15, n. 5, p. 355-360, 2009a.
- YAN, Chunze et al. Preparation and selective laser sintering of nylon-12 coated metal powders and post processing. **Journal of Materials Processing Technology**, v. 209, n. 17, p. 5785-5792, 2009b.